Proceedings of XIX International Scientific Conference "New Technologies and Achievements in Metallurgy, Material Engineering, Production Engineering and Physics", Częstochowa, Poland, June 7–8, 2018

Crystallization Studies of Hard Magnetic $Pr_9Fe_{56}Co_{13}Zr_1Ti_3B_{18}$ Alloys Ribbons of Various Thicknesses

K. Pawlik*

Institute of Physics, Częstochowa University of Technology, al. Armii Krajowej 19, 42-200 Częstochowa, Poland

The present studies are focused on the rapidly solidified ribbons of the $Pr_9Fe_{56}Co_{13}Zr_1Ti_3B_{18}$ alloy. The ribbons were obtained by melt spinning technique at various linear velocities of the copper roll surface, thus leading to their various thicknesses. The X-ray diffraction studies revealed differences in the degree of crystallinity in the as-cast state that depends on the thickness of the ribbon. It was also shown that the surface of the thickest ribbon being in contact with copper roll was amorphous while the free surface was partly crystalline. The aim of the present work was to determine the influence of the initial structural state of the ribbons on the crystallization processes during annealing. The annealing conditions were set base on the DSC studies. These structural characteristic features were used to explain the changes of magnetic properties of studied specimens.

DOI: 10.12693/APhysPolA.135.200

PACS/topics: 75.50.Ww, 75.50.Tt, 81.05.Kf, 81.07.Bc

1. Introduction

Processing nanocrystalline RE-Fe-B type magnets derived from amorphous precursors that would reveal homogeneous microstructure when subjected to annealing is a complex process requiring rigorous technological window parameters [1]. It is especially difficult in case of bulk metallic glasses as well as ribbons melt spun at low speed of copper roll, where processing may lead to their partial crystallization. Appropriate admixture of elements as Y, Cr, Zr, Ti, Nb, or B may have beneficial impact on glass forming ability of the alloys and shift of the crystallization temperature towards higher values [2, 3]. Additionally, the admixture of Zr or Nb restrains the grain growth during annealing and leads to formation of homogeneous microstructure [4]. Appropriate alloying elements can also limit the crystallization of metastable phases thus promoting the formation of hard magnetic phase [5]. In the present work the Pr–Fe–Co–Zr–Ti–B alloy ribbons melt-spun at various speed of the copper roll were studied. Variation of the copper roll velocity led to their different thicknesses and partial crystallization in the as-cast state. The aim of the work was to determine the influence of the initial state of the samples on their crystallization processes and magnetic properties.

2. Samples preparation and experimental methods

The rapidly solidified ribbons of the $Pr_9Fe_{56}Co_{13}Zr_1Ti_3B_{18}$ alloy were produced with different speed of the copper roll leading to different average thicknesses of the samples: 25 m/s — 25 μm, 10 m/s — 70 μm, 5 m/s — 140 μm. The as-cast samples were checked for the presence of crystalline phases using X-ray diffraction (XRD). The XRD studies were performed using Bruker D8 Advance diffractometer operating in the Bragg–Brentano configuration. The instrument was equipped with Cu X-ray tube with linear focus of 25 mm and the K_β filter mounted on LynxEye detector. Thermal stability parameters were determined using differential scanning calorimetry (DSC). To establish the activation energies for crystallization the DSC curves were measured in the temperature range 750–1020 K with various heating rates ($20 \leq \beta \leq 40$ K/min). Subsequently, the specimens were sealed off in the quartz tubes under the argon atmosphere and annealed for 5 min at temperatures ranging from 923 K to 1023 K. The room temperature hysteresis loops were measured using the LakeShore 7307 VSM magnetometer operating in the external magnetic fields up to 1600 kA/m.

3. Results and discussion

The diffraction spectra measured on top and bottom sides of the as-cast ribbons of various thicknesses are presented in Fig. 1. The 25 μm thick ribbon was fully amorphous on both sides of the sample. The 140 μm thick ribbon was partially crystalline on the side that did not have a direct thermal contact with the copper roll.

In Fig. 2 the hysteresis loops measured for as-cast ribbons of various thicknesses are presented. The hysteresis loops obtained for ribbons of 25 μm (25 m/s) and 70 μm (10 m/s) were typical for the soft magnetic materials, with the saturation polarization (J_s) of about 1.0 T. Minor differences in shapes of hysteresis loops might be related to different strains induced during rapid solidification. On the other hand, for the thickest sample (5 m/s) a clear change in the hysteresis loop is visible. Its wasp-wasted shape as well as a lower saturation polarisation are related to a low volume fraction of the hard magnetic crystallites embedded within the amorphous matrix (as was shown in Fig. 1).

*e-mail: kpawlik@wip.pcz.pl

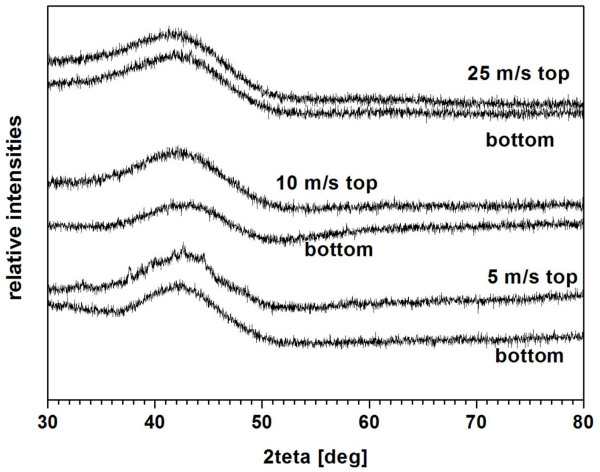

Fig. 1. The XRD patterns for $Pr_9Fe_{56}Co_{13}Zr_1Ti_3B_{18}$ alloy as-cast ribbons measured at the bottom and top side of the samples.

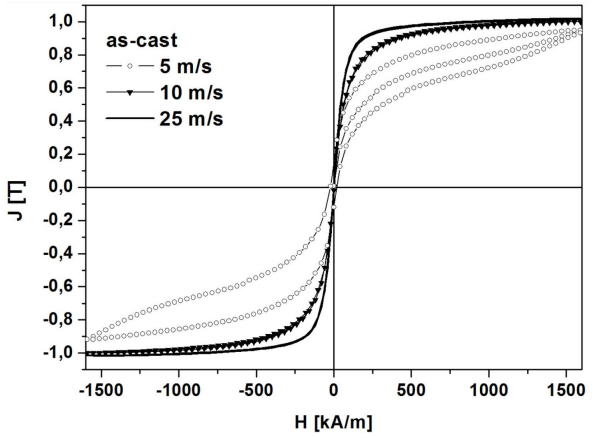

Fig. 2. The hysteresis loops measured for $Pr_9Fe_{56}Co_{13}Zr_1Ti_3B_{18}$ alloy as-cast ribbons of various thicknesses.

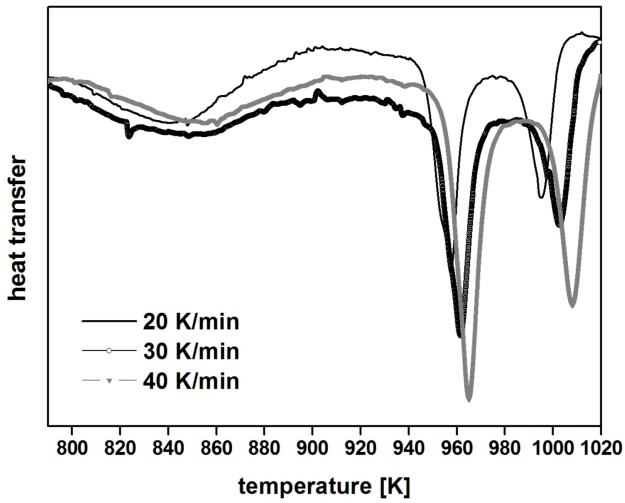

Fig. 3. DSC curves for $Pr_9Fe_{56}Co_{13}Zr_1Ti_3B_{18}$ alloy amorphous ribbons measured at different heating rates.

The DSC scans measured with different heating rates β = 20, 30, and 40 K/min for the amorphous ribbon sample (25 m/s) are presented in Fig. 3. One can observe the step on each curve that reflects the glass transition of the alloy and two well separated crystallization peaks. For the heating rate 20 K/min the glass transition temperature (T_g = 848 K) and the crystallization peak temperatures (T_{p1} = 958 K and T_{p2} = 996 K) were determined. Additionally, the onset crystallization temperature (T_{x1} = 948 K) and the supercooled liquid region ($\Delta T_x = T_{x1} - T_g$ = 100 K) were calculated. Using the Kissinger method the effective activation energies E_a for crystallization were determined for both crystallization peaks (E_{a1} = 703 kJ/mol and E_{a2} = 420 kJ/mol). It is worth mentioning that the activation energy E_{a1} takes a very high value indicating the high temperature stability of the amorphous phase for this alloy.

Subsequently the ribbons of various thicknesses were annealed at temperatures ranging from 923 K to 1023 K for 5 min and examined with XRD. In case of the thickest ribbons (5 m/s), for which the top side was partly crystalline in the as-cast state, the diffraction patterns were measured for both: the top and bottom sides (Fig. 4).

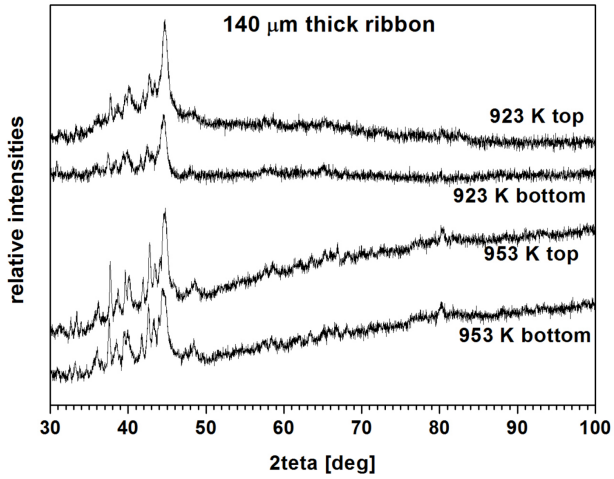

Fig. 4. The diffraction patterns for 140 μm thick ribbons annealed at various temperatures measured for top and bottom sides.

It turned out that the differences in the state of crystallinity disappear after annealing of the samples. The only difference is the greater relative intensity of the peak attributed to the α-Fe phase, which is slightly higher for the top surface of the ribbon, i.e. for the surface that was initially partly crystalline. However, for both surfaces, the same crystalline phases are identified. Phase analysis revealed presence of hard magnetic $Pr_2(Fe,Co)_{14}B$, paramagnetic $Pr_{1+x}Fe_4B_4$ and soft ferromagnetic α-Fe phases.

The hysteresis loops measured for the samples of various thicknesses subjected to annealing are presented in Fig. 5. Corresponding magnetic parameters are also collected in Table I.

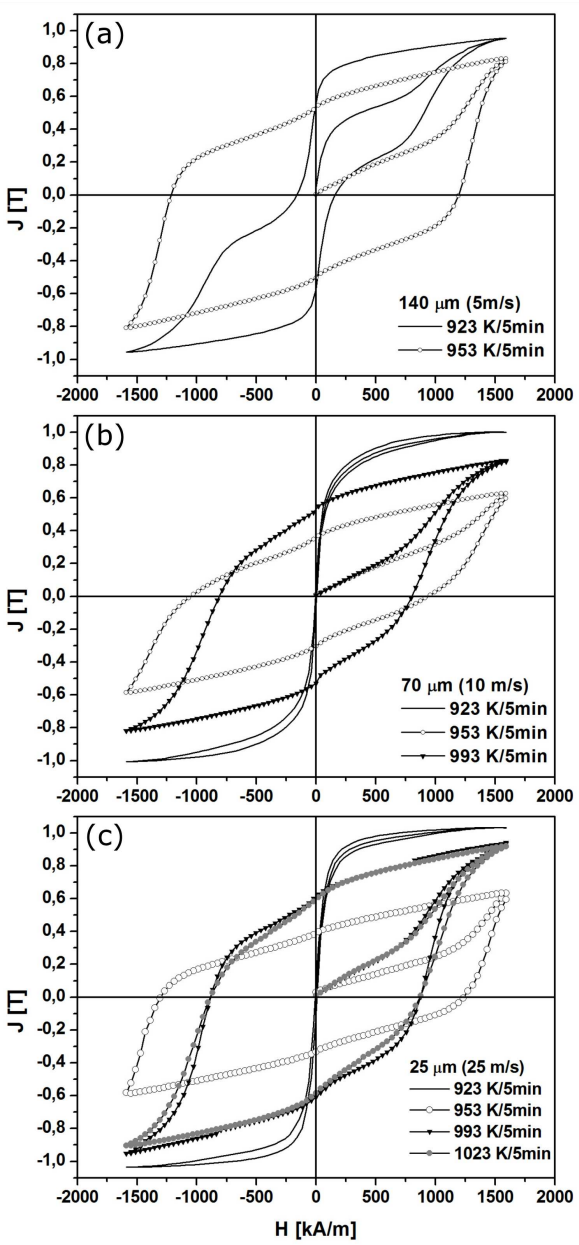

Fig. 5. The hysteresis loops measured for 140 μm (a), 70 μm (b) and 25 μm (c) thick ribbons annealed at various temperatures.

Annealing of 25 μm and 70 μm thick ribbons at 923 K does not cause significant changes in shapes of hysteresis loops. However in case of 140 μm thick ribbon a significant change of magnetic properties was observed due to a growth of crystallites nucleated during rapid solidification. The highest coercivities ${}_JH_c$ were measured for ribbons annealed at 953 K in all cases, although ${}_JH_c$ reached the highest value for 25 μm thick ribbon. Annealing at higher temperatures resulted in decrease of the coercive field, but the highest maximum magnetic energy product $(BH)_{\max}$ reaching 53 kJ/m^3 was measures for the 25 μm thick ribbon annealed at 993 K.

TABLE I

The magnetic parameters values for ribbons of various thicknesses annealed at different temperatures (${}_JH_c$ — coercivity, J_s — saturation magnetization, J_r — remanence, $BH_{\max}$ — maximum energy product).

	${}_JH_c$ [kA/m]	J_s [T]	J_r [T]	$BH_{\max}$ [kJ/m^3]
140 μm				
923 K	160	0.95	0.56	10
953 K	1190	0.82	0.53	41
70 μm				
923 K	10	1.00	0.05	–
953 K	1027	0.63	0.33	19
993 K	820	0.83	0.53	40
25 μm				
923 K	7	1.03	0.1	–
953 K	1309	0.63	0.39	24
993 K	875	0.93	0.61	53
1023 K	866	0.92	0.59	48

4. Conclusions

It was shown that the rapid solidification of the $Pr_9Fe_{56}Co_{13}Zr_1Ti_3B_{18}$ alloy at low cooling rate (5 m/s) results in crystallization of top surface of the ribbon. Its further annealing at 923 K causes growth of crystallites and significant change of magnetic properties. Although the phase constitution does not depend on the state of crystallinity, relative intensities of peaks (especially attributed to α-Fe) differ for top and bottom surface of the sample. For fully amorphous samples (25 μm and 70 μm thick ribbons), a development of hard magnetic properties is possible when annealed at 950 K due to high activation energy for crystallization. The best magnetic properties were obtained for 25 μm thick ribbon annealed at temperatures higher than 923 K. Slightly inferior magnetic properties of 70 μm thick ribbon might be related to lower heat transfer for thicker ribbons during short time annealing.

References

[1] I. Betancourt, H.A. Davies, *J. Magn. Magn. Mater.* **261**, 328 (2003).

[2] W.Y. Zhang, C.H. Chiu, L.C. Zhang, K. Biswas, H. Ehrenberg, W.C. Chang, J. Eckert, *J. Magn. Magn. Mater.* **308**, 24 (2007).

[3] K. Pawlik, P. Pawlik, J.J. Wysłocki, *Acta Phys. Pol. A* **118**, 900 (2010).

[4] C. Wang, M. Yan, W.Y. Zhang, *Mater. Sci. Eng. B* **123**, 80 (2005).

[5] W.W. Yang, J. Luo, H.-J. Peng, Y.-L. Sui, X.-X. Gao, *Rare Met.* **33**, 171 (2014).